

**Two distinct superconducting fluctuation diamagnetisms in  $\text{Bi}_2\text{Sr}_{2-x}\text{La}_x\text{CuO}_{6+\delta}$** H. Xiao,<sup>1</sup> T. Hu,<sup>2,\*</sup> W. Zhang,<sup>1,3</sup> Y. M. Dai,<sup>1</sup> H. Q. Luo,<sup>1</sup> H. H. Wen,<sup>4</sup> C. C. Almasan,<sup>5</sup> and X. G. Qiu<sup>1</sup><sup>1</sup>*Beijing National Laboratory for Condensed Matter Physics, Institute of Physics, Chinese Academy of Sciences, Beijing 100190, China*<sup>2</sup>*State Key Laboratory of Functional Materials for Informatics, Shanghai Institute of Microsystem and Information Technology, Chinese Academy of Sciences, Shanghai 200050, China*<sup>3</sup>*School of Physical Science and Technology & Collaborative Innovation Center of Suzhou Nano Science and Technology, Soochow University, Suzhou 215006, China*<sup>4</sup>*Department of Physics, Nanjing University, Nanjing 210093, China*<sup>5</sup>*Department of Physics, Kent State University, Kent, Ohio 44240, USA*

(Received 16 October 2013; revised manuscript received 18 September 2014; published 8 December 2014)

Superconducting fluctuations were studied through angular-dependent torque measurements on a series of  $\text{Bi}_2\text{Sr}_{2-x}\text{La}_x\text{CuO}_{6+\delta}$  (BSLCO) single crystals. Two distinct superconducting fluctuation diamagnetisms were observed: one is the superconducting thermal fluctuation, with a boundary close to the superconducting phase boundary, while the other one, up to a temperature as high as about 180 K, showing maximum signal in the sample with hole carrier density  $p = 0.125$ , could be due to preformed pairs. In addition, we observed linearly temperature-dependent paramagnetic torque signals in BSLCO samples, possibly a result of quantum criticality from a quantum critical point at the optimal doping.

DOI: [10.1103/PhysRevB.90.214511](https://doi.org/10.1103/PhysRevB.90.214511)

PACS number(s): 74.25.Dw, 74.25.Uv, 74.40.Kb, 74.72.Kf

The study of superconducting fluctuations in cuprates attracts a lot of interest since we may underestimate the superconducting transition temperature  $T_c$  due to the effect of these fluctuations. There is growing evidence for the existence of a superconducting fluctuation signal above the superconducting transition temperature  $T_c$  in cuprates. For example, a large Nernst effect and diamagnetism are observed, which suggest the presence of a vortex liquid state far above  $T_c$  [1,2]. However, specific heat measurements [3] and terahertz spectroscopy [4] show that the fluctuations persist near  $T_c$  in a narrow temperature range. Since reports from the literature show remarkably different temperature ranges, a question that remains open is the exact boundary of the superconducting fluctuations. Some believe that, although the reported onset temperature of superconducting fluctuations is already high above  $T_c$ , this merely marks the point at which instruments lose sensitivity in detecting phase fluctuations, which may remain important up to the much higher pseudogap temperature [5].

Furthermore, the origin of the fluctuations is also in debate. For example, it is claimed that the field-enhanced diamagnetic signal  $M$  above the transition temperature  $T_c$  in  $\text{Bi}_2\text{Sr}_2\text{CaCu}_2\text{O}_{8+\delta}$  can distinguish  $M$  from conventional amplitude fluctuations and support the vortex scenario for the loss of phase coherence at  $T_c$ ; while in Ref. [6] it is shown that this result can also be explained on the basis of the conventional Ginzburg-Landau scenario. Scanning tunneling microscopy measurements visualized nanometer-sized pairing regions in  $\text{Bi}_2\text{Sr}_2\text{CaCu}_2\text{O}_{8+\delta}$  [7], thus providing microscopic evidence for a preformed pairing origin for the fluctuating superconducting response. Although great efforts have been made to investigate this matter, the origin and exact boundary of the superconducting fluctuations are still interesting but controversial problems and require further study.

Magnetic torque is a sensitive tool to detect the presence of vortices. The angular-dependent technique has advantages over the fixed-angle method, since it is easy to eliminate the angular-independent background more completely, and hence more reliable results are obtained. Moreover, one can obtain more information about superconducting fluctuation diamagnetism through this technique, since the Abrikosov vortex lattice shows special angular-dependent torque behavior [8]. In this paper, we investigate the superconducting fluctuation diamagnetism through angular-dependent torque measurements on a series of  $\text{Bi}_2\text{Sr}_{2-x}\text{La}_x\text{CuO}_{6+\delta}$  (BSLCO) single-crystal samples and observe a precursor superconducting state which survives up to  $T_c^{\text{onset}}$ , as high as about 180 K. Instead, the Abrikosov vortex disappears at  $T_c'$ , which is above but very close to  $T_c$ . Thus, we identify three different regions in the superconducting phase. Region I is characterized by superconductivity (SC) with long-range phase coherence. In region II, the SC has lost long-range phase coherence but Abrikosov vortices are still present. In region III, superconducting fluctuations extends to very high temperatures and show a maximum in the sample with carrier density  $p = 0.125$ , possibly due to preformed Cooper pairs. In addition, the existence of a quantum critical point (QCP) is evidenced by a slope change of the temperature-dependent torque curve in the paramagnetic state.

Single crystals of  $\text{Bi}_2\text{Sr}_{2-x}\text{La}_x\text{CuO}_{6+\delta}$ , with nominal doping  $x = 0.1, 0.2, 0.4, 0.6, 0.7$ , and  $0.8$  were grown using the traveling-solvent floating-zone technique [9]. The corresponding hole doping concentration  $p$  is 0.19, 0.184, 0.16, 0.129, 0.115, and 0.109, according to Ref. [10]. We determine  $T_c$  for each doping using a superconducting quantum interference design magnetometer. The temperature-dependent magnetization measurements were done in a magnetic field  $H$  of 10 Oe, applied parallel to the  $ab$  plane of the single crystal. The doping dependence of the  $T_c$  obtained is summarized in Fig. 1(d) (open circles). The magnetic torque experienced by a sample of magnetic moment  $M$  in an applied magnetic field  $H$  was measured over a wide temperature range from 10 to 300 K and

\*Author to whom correspondence should be addressed: [thu@mail.sim.ac.cn](mailto:thu@mail.sim.ac.cn)

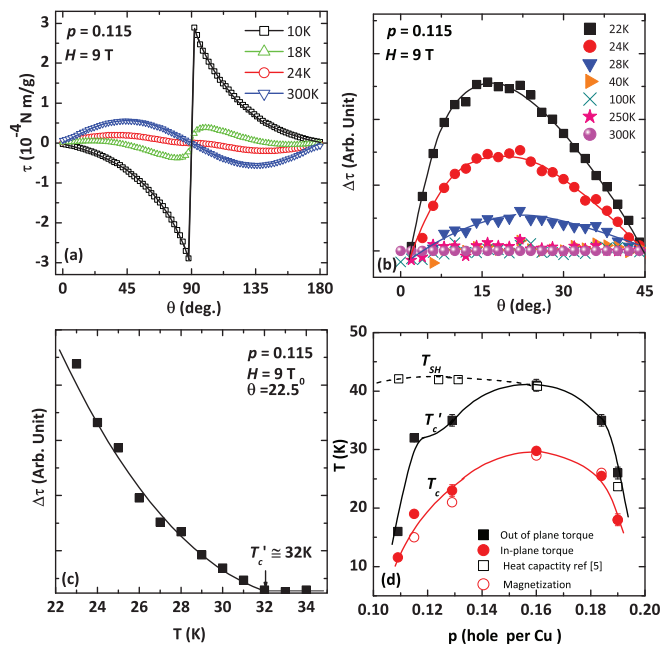


FIG. 1. (Color online) Data for BSLCO sample with hole concentration  $p = 0.115$ . (a) Angular- ( $\theta$ )- dependent torque  $\tau$  measured at temperatures  $T = 10, 18, 24$ , and  $300$  K with a magnetic field  $H = 9$  T. Solid lines are fitting curves for the  $T = 10$  K and  $300$  K data, respectively. (b)  $\Delta\tau \equiv \tau(\theta) - \tau(90^\circ - \theta)$  vs  $\theta$  for temperatures  $T = 22, 24, 28, 40, 100, 250$ , and  $300$  K. (c)  $\Delta\tau$  vs  $T$  for the fixed angle  $\theta = 22.5^\circ$ . (d) Doping dependence of characteristic temperatures  $T_c$ ,  $T'_c$ , and  $T_{SH}$ .  $T_c$  is the superconducting transition temperature obtained from magnetization ( $\circ$ ) and in-plane torque ( $\bullet$ ) measurements;  $T'_c$  is the temperature up to which the Abrikosov vortices survive, extracted from out-of-plane torque measurements ( $\blacksquare$ , present work);  $T_{SH}$  is the temperature up to which residual superconductivity survives, obtained from specific heat measurements ( $\square$ , Ref. [3]).

with  $H$  up to  $9$  T using a piezoresistive torque magnetometer in a physical property measurement system. Both out-of-plane and in-plane torque measurements were performed, and for the out-of-plane rotation, the angle  $\theta$  is defined as the angle between the magnetic field and the  $c$  axis of the single crystal.

Figure 1(a) shows  $\tau(\theta)$  measured on the  $p = 0.115$  BSLCO sample at  $10, 18, 24$ , and  $300$  K with  $H = 9$  T. The  $300$  K data (blue symbols) are typical for a pure paramagnetic signal [11] (the blue solid line is a fitting curve for  $\tau_0 \sin 2\theta$ ). The  $10$  K data represent a typical Abrikosov vortex torque signal, and can be well fitted (black curve) by Kogan's model, which is derived in the frame of the anisotropic Ginzburg-Landau regime:  $\tau_v(\theta) = \frac{\phi_0 H V}{16\pi\mu_0\lambda^2} \frac{\gamma^2 - 1}{\gamma} \frac{\sin 2\theta}{\epsilon(\theta)} \ln\left\{\frac{\gamma\eta H_{c2}}{H\epsilon(\theta)}\right\}$ , where  $V$  is the sample volume,  $\phi_0$  is the flux quantum,  $\mu_0$  is the vacuum permeability,  $\lambda$  is the penetration depth in the  $ab$  plane,  $\gamma$  is the anisotropy parameter,  $\epsilon(\theta) = (\sin^2\theta + \gamma^2 \cos^2\theta)^{1/2}$ ,  $\eta$  is a numerical parameter of the order of unity, which accounts for the structure of the vortex core, and  $H_{c2}$  is the upper critical field parallel to the  $c$  axis. This equation reflects the presence of Abrikosov vortices in an anisotropic superconductor.

The  $\tau(\theta)$  at  $18$  and  $24$  K in Fig. 1(a) incorporate both the  $\sin 2\theta$  term and Abrikosov vortex torque signals. To determine how the Abrikosov vortex signal evolves and the

exact temperature at which it disappears, we get rid of the torque of the  $\sin 2\theta$  term by asymmetrizing the  $\tau(\theta)$  with respect to  $45^\circ$ , that is,  $\Delta\tau \equiv \tau(\theta) - \tau(90^\circ - \theta)$ . Figure 1(b) plots the angular ( $\theta$ ) dependence of  $\Delta\tau$  for temperatures  $T$  from  $22$  to  $300$  K. It is found that the amplitude of the torque signal is getting smaller with increasing temperature and for high temperatures ( $T \geq 40$  K),  $\Delta\tau$  is scattered, suggesting the vanishing of the Abrikosov vortex torque. To determine the exact vanishing temperatures, we plot  $\Delta\tau$  vs  $T$  for fixed angle  $\theta = 22.5^\circ$ ; see Fig. 1(c). Note that  $\Delta\tau$  decreases with increasing temperature and vanishes at  $T'_c = 32$  K, which is higher than the superconducting transition temperature of this sample,  $T_c = 15$  K, as determined by magnetization measurements. Similar analyses were applied to all the samples and the hole-carrier-concentration- ( $p$ )-dependent  $T'_c$ 's are summarized in Fig. 1(d), where all  $T'_c$ 's ( $\blacksquare$ ) are higher compared with the corresponding  $T_c$ 's ( $\circ$ , determined by magnetization measurements). We also performed angular-dependent in-plane torque measurements (data not shown) and found that  $\tau^{ab}$  vanishes [ $\bullet$ , Fig. 1(d)] when approaching  $T_c$ . It is found that the  $T_c$  values determined from different measurements are consistent. As discussed in our previous work, the vanishing of  $\tau^{ab}$  actually suggests the loss of long-range phase coherence at  $T_c$  [12].

The open squares in Fig. 1(d) are the temperatures  $T_{SH}$ , determined by specific heat measurements, up to which residual superconductivity persists [3].  $T'_c$  and  $T_{SH}$  overlap in the overdoped region, but they deviate from each other in the underdoped region. The difference between  $T_{SH}$  and  $T'_c$  could have three possible causes. First of all, the specific heat detects the entropy reduction due to preformed pairing [3], which does not determine whether the vortex system consists of Abrikosov vortices or spontaneous vortex excitations due to residual Cooper pairs. Second, the resolution of the specific heat may be much lower than the torque measurements. Third, the specific heat measurements may not be able to distinguish the superconducting order from the charge order which is present at  $p = 1/8$  [13–15] in cuprates, while our angular-dependent torque measurements are particularly for detection of vortex excitations.

For temperatures higher than  $T'_c$ , all the torque data display a  $\sin 2\theta$  angular dependence. Figure 2(a) shows the  $T$ -dependent torque with  $H = 9$  T for all doped samples from  $p = 0.109$  to  $p = 0.19$ . Note that  $\tau_0$  is the coefficient before  $\sin 2\theta$  when the angular-dependent torque data for  $T > T'_c$  are fitted. We found that for all samples, the torque signal is almost linear at high temperatures (see the dashed lines), and it shows a sharp decrease at low temperatures due to superconducting fluctuations. Figure 2(b) shows  $\tau_0/H$  vs  $H$  for the  $p = 0.115$  sample at  $T = 100$  K (blue circles) and  $300$  K (red diamonds). These two temperatures correspond to the high-temperature  $T$ -linear region and the low-temperature superconducting fluctuation region, respectively.  $\tau_0/H$  at  $300$  K increases linearly with  $H$  and approaches  $0$  at zero magnetic field, which is a typical paramagnetic torque behavior  $\tau_p \propto H^2$  [since  $\tau_p = 1/2(\chi_c - \chi_a)H^2 \sin 2\theta$ ]. However,  $\tau_0/H$  at  $100$  K shows different behavior, changing sign from positive to negative when approaching zero magnetic field, which suggests that the superconducting fluctuation diamagnetism dominates at low magnetic field.

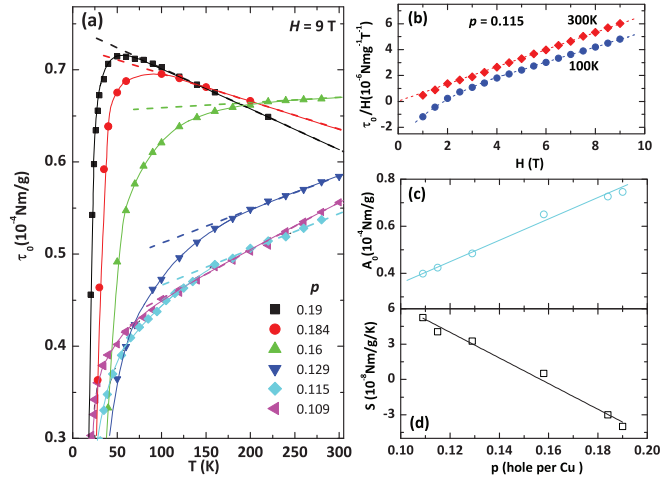


FIG. 2. (Color online) (a) Temperature- ( $T$ )- dependent out-of-plane torque  $\tau_0$  for BSLCO samples with  $p = 0.109, 0.115, 0.129, 0.16, 0.184,$  and  $0.19$ . The dashed lines are linear fits of the high-temperature part of the torque data. (b) Magnetic field ( $H$ ) dependence of  $\tau_0/H$  at  $T = 100$  K (blue solid circles) and  $300$  K (red solid diamonds) for the BSLCO sample with  $p = 0.115$ . (c) and (d) are the  $p$  dependence of the zero-temperature torque  $A_0$  and the slope  $S$ , respectively, which are the fitting result for the high-temperature part of the torque data in the fitting function  $\tau_0 = A_0 + ST$ .

We fit the the high-temperature  $\tau_0$  with  $\tau_0 = A_0 + ST$  and plot the  $p$  dependence of the intercept  $A_0$  and slope  $S$  in Figs. 2(c) and 2(d), respectively. It was found that  $A_0$  shows a linear behavior with  $p$  [Fig. 2(c)] which gives  $A_0 \propto (p - 0.01)$ ; while the slope  $S \propto (p - p^*)$  with  $p^* = 0.159 \pm 0.01$  changes sign with increasing doping, from positive to negative, and for the  $p = 0.16$  sample, the slope is zero [Fig. 2(d)]. The linear temperature dependence of the torque in the high-temperature region could be a result of quantum criticality. The reason is the following. Torque is associated with the free energy  $F$  of the system, that is,  $\tau = -\partial F/\partial\theta$ . The quantum critical scaling for the free energy  $F$  indicates that  $F$  is of the order of the thermal energy  $k_B T$  per correlated volume  $\xi^d$  (where  $k_B$  is the Boltzman constant,  $\xi$  is the correlation length, and  $d$  is the spatial dimension), that is,  $F \sim k_B T \xi^{-d} \sim k_B T (p - p^*)^{-d}$  (see Ref. [16]), where  $p$  is the tuning parameter,  $p^*$  is the quantum critical point, and  $v$  is the correlation-length exponent. In our case,  $F(T) \propto \tau \propto T(p - p^*)$ . So we have  $dv = 1$ . For the case of  $d = 2$ , it follows that  $v = 1/2$ , which is consistent with the standard Hertz-Millis-Moriya type of quantum criticality [17]. So the high-temperature torque data suggest that the QCP at the optimal doping dominates the thermodynamics in the high-temperature region. The presence of a QCP at optimal doping in BSLCO is also evidenced by Hall effect [18] and resistivity [10] measurements. The quantum phase transition at the exact location of  $p$  that maximizes  $T_c$  might be a universal feature of cuprates [19,20]. Our torque measurement results show that quantum fluctuations from this QCP dominate thermodynamic properties up to surprisingly high temperature.

Note that linear temperature- ( $T$ )- dependent susceptibility was previously observed [21] in  $\text{Bi}_2\text{Sr}_2\text{CaCu}_2\text{O}_{8+\delta}$ , and was attributed to Pauli paramagnetism,  $\chi_P =$

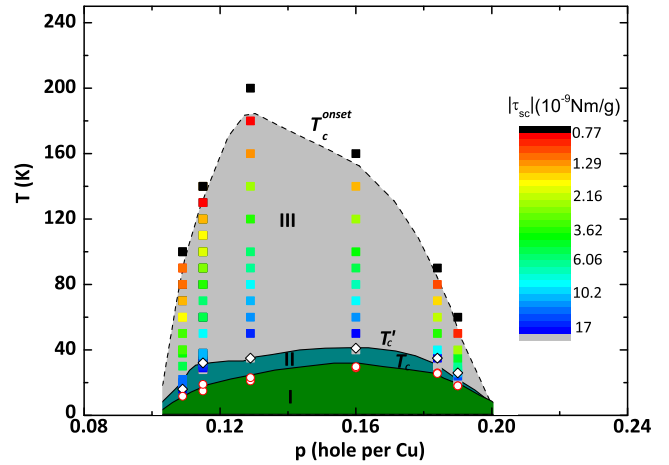


FIG. 3. (Color online) Phase diagram for the hole carrier density  $p$  vs temperature  $T$  for BSLCO. Region I is the superconducting phase with long-range phase coherence. Region II is the superconducting thermal fluctuation region. Region III is the region where the superconduction fluctuation is from preformed pairs. The intensity of  $|\tau_{sc}|$  is plotted on a logarithmic scale and shows a maximum at  $p = 0.125$  for all the temperatures in region III.

$\mu_B^2 \int_0^\infty (-df/dE)g(E)dE$ , where  $g(E)$  is the density of state (DOS) and  $f$  is the Fermi function.  $\chi_P$  is temperature independent if the smearing of the Fermi surface due to finite temperature is ignored; however, if temperature is included, there will be a small correction term which is proportional to  $T^2$ . Since  $\chi_P$  reflects the thermally averaged DOS near  $E_F$ , the observed abnormal linear  $T$  dependence of  $\chi_P$  can be explained by the anomalous energy-dependent DOS and its doping evolution [21,22]. In our case of BSLCO, the linear  $T$ -dependent susceptibility behavior could be due to quantum criticality affecting the DOS.

We did further analysis by subtracting the high-temperature linear part in the data of Fig. 2(a) to obtain the torque  $\tau_{sc}$ , which has a negative value below a characteristic temperature  $T_c^{\text{onset}}$ . The negative value suggests the presence of a superconducting diamagnetic signal [1]. For  $T$  below  $T_c^{\text{onset}}$ , but above  $T_c'$ , we plot  $|\tau_{sc}|$  as a contour plot in the temperature-doping ( $T$ - $p$ ) phase diagram of BSLCO (see Fig. 3, where data points with the same color have the same value of  $|\tau_{sc}|$ ).

From the different characters of our torque data, we found that the superconducting phase has three different regions I, II, and III, shown with colors in Fig. 3. Region I (green) is the superconducting phase with long-range phase coherence. Region II (blue) gives the upper boundary of  $T_c'$ , as determined in Fig. 1(d). The vortex matter in region II is still well described by the Ginzberg-Landau theory, although the superconductor has lost long-range coherence. Therefore, the superconducting fluctuation in the vicinity of the critical temperature (region II) can be described within the framework of Ginzberg-Landau theory: thermodynamic fluctuations give rise to the superconducting effect for  $\langle\psi^2\rangle \neq 0$  although  $\langle\psi\rangle = 0$ , where  $\psi$  is the classical bosonic field in Ginzberg-Landau theory [23].

A diamagnetic signal from superconducting fluctuations is also observed in region III (the gray region). In this region, the diamagnetic signal is different from the one

in region II, since the former can be fitted by a  $\sin 2\theta$  dependence while the latter can be fitted by Kogan's model. In addition, it shows the strongest superconducting diamagnetism fluctuation (largest  $|\tau_{sc}|$ ) at  $p = 0.125$  for all temperatures  $T > T'_c$ , while for superconducting thermal fluctuations, the strongest diamagnetism fluctuation should be present at the doping level which maximizes  $T_c$ . Since the strongest stripe pattern was also observed at  $p = 0.125$  in cuprates [24], this suggests the close relationship between the superconducting fluctuation diamagnetism and the stripe order. This observation is consistent with the result from scanning tunneling microscopy experiment that the striped state at  $p = 0.125$  comes from preformed uncondensed Cooper pairs forming spin-charge ordered structures [25]. Therefore, the superconducting diamagnetism fluctuation in region III could be from preformed uncondensed Cooper pairs. This may suggest that a different type of vortex excitation, probably spontaneous vortex excitation, is present in region III, not the conventional Abrikosov vortex [26].

In summary, we identified two distinct superconducting fluctuation diamagnetisms above  $T_c$  by angular-dependent torque measurements: superconducting thermal fluctuations

up to  $T'_c$  in region II and superconducting fluctuations from preformed pairs up to  $T_c^{\text{onset}}$  in region III. The observation of two distinct superconducting fluctuation boundaries may reconcile the discrepancies regarding the origin and the exact boundary of the fluctuations since the different techniques may be sensitive to one type of fluctuation but not the other. In addition, we show that the quantum criticality from the quantum critical point in an optimally doped BSLCO sample could give the linearly temperature-dependent paramagnetic torque.

We sincerely thank Professor Zhi-Xun Shen from Stanford University and Professor Dunghai Lee from the University of California, Berkeley for intuitive discussions and valuable comments and suggestions with regard to the preparation of this manuscript. The work at IOP is supported by MOST of China, Projects No. 2011CBA00107 and No. 2012CB921302 and NSFC, Project No. 11104335. T.H. is supported by the Strategic Priority Research Program (B) of the Chinese Academy of Sciences Grant No. XDB04040300. C.C.A. is supported by NSF Grants No. DMR-1006606 and No. DMR-0844115 and the ICAM Branches Cost Sharing Fund from the Institute for Complex Adaptive Matter.

- 
- [1] Y. Wang, L. Li, M. J. Naughton, G. D. Gu, S. Uchida, and N. P. Ong, *Phys. Rev. Lett.* **95**, 247002 (2005).
  - [2] L. Li, Y. Wang, S. Komiya, S. Ono, Y. Ando, G. D. Gu, and N. P. Ong, *Phys. Rev. B* **81**, 054510 (2010).
  - [3] H.-H. Wen, G. Mu, H. Luo, H. Yang, L. Shan, C. Ren, P. Cheng, J. Yan, and L. Fang, *Phys. Rev. Lett.* **103**, 067002 (2009).
  - [4] L. S. Bilbro, R. V. Aguilar, G. Logvenov, O. Pelleg, I. Bozovic, and N. P. Armitage, *Nat. Phys.* **7**, 298 (2011).
  - [5] M. Franz, *Nat. Phys.* **3**, 686 (2007).
  - [6] L. Cabo, J. Mosqueira, and F. Vidal, *Phys. Rev. Lett.* **98**, 119701 (2007).
  - [7] K. K. Gomes, A. N. Pasupathy, A. Pushp, S. Ono, Y. Ando, and A. Yazdani, *Nature (London)* **447**, 569 (2007).
  - [8] V. G. Kogan, *Phys. Rev. B* **38**, 7049 (1988).
  - [9] H. Luo, P. Cheng, L. Fang, and H.-H. Wen, *Supercond. Sci. Technol.* **21**, 125024 (2008).
  - [10] Y. Ando, Y. Hanaki, S. Ono, T. Murayama, K. Segawa, N. Miyamoto, and S. Komiya, *Phys. Rev. B* **61**, R14956 (2000).
  - [11] H. Xiao, T. Hu, C. C. Almasan, T. A. Sayles, and M. B. Maple, *Phys. Rev. B* **73**, 184511 (2006).
  - [12] T. Hu, H. Xiao, P. Gyawali, H. H. Wen, and C. C. Almasan, *Phys. Rev. B* **85**, 134516 (2012).
  - [13] P. Dai, H. A. Mook, and F. Doğan, *Phys. Rev. Lett.* **80**, 1738 (1998).
  - [14] M. Akoshima, T. Noji, Y. Ono, and Y. Koike, *Phys. Rev. B* **57**, 7491 (1998).
  - [15] H. E. Mohottala, *Nat. Mater.* **5**, 377 (2006).
  - [16] C. Varma, Z. Nussinov, and W. van Saarloos, *Phys. Rep.* **361**, 267 (2002).
  - [17] H. v. Löhneysen, A. Rosch, M. Vojta, and P. Wölfle, *Rev. Mod. Phys.* **79**, 1015 (2007).
  - [18] F. F. Balakirev, J. B. Betts, A. Migliori, S. Ono, Y. Ando, and G. S. Boebinger, *Nature (London)* **424**, 912 (2003).
  - [19] X. F. Sun, S. Komiya, J. Takeya, and Y. Ando, *Phys. Rev. Lett.* **90**, 117004 (2003).
  - [20] F. F. Balakirev, J. B. Betts, A. Migliori, I. Tsukada, Y. Ando, and G. S. Boebinger, *Phys. Rev. Lett.* **102**, 017004 (2009).
  - [21] T. Watanabe, T. Fujii, and A. Matsuda, *Phys. Rev. Lett.* **84**, 5848 (2000).
  - [22] G. V. M. Williams, J. L. Tallon, R. Michalak, and R. Dupree, *Phys. Rev. B* **57**, 8696 (1998).
  - [23] M. Tinkham, *Introduction to Superconductivity* (Mineola, New York, 2004), p. 287.
  - [24] C. V. Parker, P. Aynajian, E. H. da Silva Neto, A. Pushp, S. Ono, J. Wen, Z. Xu, G. Gu, and A. Yazdani, *Nature (London)* **468**, 677 (2010).
  - [25] T. Valla, A. V. Fedorov, J. Lee, J. C. Davis, and G. D. Gu, *Science* **314**, 1914 (2006).
  - [26] P. W. Anderson, *Nat. Phys.* **3**, 160 (2007).